Proprotein Convertase Subtilisin/Kexin Type 9 Deficiency Reduces Melanoma Metastasis in Liver[1,2]

Xiaowei Sun*, Rachid Essalmani*, Robert Day[†], Abdel M. Khatib[‡], Nabil G. Seidah* and Annik Prat*

*Laboratory of Biochemical Neuroendocrinology, Clinical Research Institute of Montreal, University of Montreal, Montreal, QC, Canada; [†]Institut de Pharmacologie de Sherbrooke, Université de Sherbrooke, Sherbrooke, QC, Canada; [‡]INSERM U1029, Université Bordeaux 1, Talence, France

Abstract

High circulating cholesterol is associated with hypercholesterolemia, atherosclerosis, and stroke. However, the relation between cholesterol and tumorigenesis/metastasis is controversial. The proprotein convertase subtilisin/kexin type 9 (PCSK9) regulates low-density lipoprotein cholesterol homeostasis by targeting the low-density lipoprotein receptor (LDLR) for degradation. PCSK9 is mostly expressed in liver, which is one of the most common sites for metastatic disease. To reveal the function of PCSK9 and also evaluate the impact of cholesterol in liver metastasis development, B16F1 melanoma cells were injected into wild-type (WT) and $Pcsk9^{-/-}$ mice to induce liver metastasis. On chow diet, $Pcsk9^{-/-}$ mice harbored two-fold less liver metastases than WT mice. This decrease is related to low cholesterol levels in $Pcsk9^{-/-}$ mice, as the protection was lost after normalizing $Pcsk9^{-/-}$ cholesterol levels by a 2-week high cholesterol diet. Furthermore, a prolongation of this diet strongly increased metastasis in both genotypes, suggesting that high cholesterol levels promote metastatic progression. The protective effect of the PCSK9 deficiency is also associated with increased apoptosis in liver stroma and metastases. Tumor necrosis factor–α (TNFα) mRNA and protein were, respectively, higher in liver stroma and plasma of injected mice, likely increasing the apoptotic TNFα signaling. Furthermore, the anti-apoptotic factor B-cell lymphoma 2 was downregulated. TNFα regulation is LDLR-independent, as its mRNA level was similarly upregulated in mice lacking both PCSK9 and LDLR. Our findings show that PCSK9 deficiency reduces liver metastasis by its ability to lower cholesterol levels and by possibly enhancing TNFα-mediated apoptosis.

Neoplasia (2012) 14, 1122–1131

Introduction

Proprotein convertase subtilisin/kexin type 9 (PCSK9) belongs to a family of secretory serine proteases, named proprotein convertases (PCs) [1]. Gain-of-function mutations in the *PCSK9* gene are associated with familial hypercholesterolemia [2]. In contrast, loss-of-function mutations are associated with reduced low-density lipoprotein cholesterol (LDLc) and lower risk of coronary artery disease [3,4]. PCSK9 regulates cholesterol homeostasis by controlling the protein levels of the low-density lipoprotein receptor (LDLR), which uptakes low-density lipoprotein particles into cells. Binding of PCSK9 to cell surface LDLR promotes its internalization and degradation in endosomal/lysosomal compartments [5–7]. PCSK9 inhibition therefore emerged as a promising therapy to treat hypercholesterolemia [8].

Beyond its role in maintaining cholesterol homeostasis, PCSK9 is implicated in numerous biologic processes. Microarray studies revealed that PCSK9 overexpression leads to the dysregulation of many pathways, including cell cycle, apoptosis, and inflammatory and stress responses [9,10]. *In vivo* studies also suggest that PCSK9 is implicated in these processes [11,12]. Following partial hepatectomy, *Pcsk9$^{-/-}$* mice exhibit a delay in hepatocyte proliferation and enhanced apoptosis, which can be rescued by feeding mice a high cholesterol diet (HCD) [11]. Moreover, *Pcsk9$^{-/-}$* mice exhibit hypoinsulinemia, hyperglycemia, and glucose intolerance [12].

Because biologic processes such as cell cycle and proliferation are modified in cancer, we suspected that PCSK9 could regulate tumorigenesis/metastasis. Furthermore, as PCSK9 inhibitors or silencers may soon be available on the market [8], it was of interest to evaluate the safety of PCSK9 deficiency in relation to cancer/metastasis. So far, only two human studies examined a possible link between PCSK9 polymorphisms known to lower circulating LDLc levels and the risk of cancer [13,14]. Although one of the studies established a statistically valid association between low circulating LDLc and increased risk of cancer [13], neither study could associate heterozygote PCSK9 loss-of-function variants (R46L, −15% LDLc; Y142X or C679X, −29% LDLc) with a higher cancer incidence. Using our PCSK9 knockout mouse models [11,15], we directly addressed the function of PCSK9 in cancer development.

In this study, upon injection of B16F1 mouse melanoma cells into spleen, which preferentially metastasize to the liver [16], *Pcsk9$^{-/-}$* mice developed less hepatic metastatic melanomas. This protective effect of the PCSK9 deficiency was abrogated by increased total cholesterol (TC) levels following an HCD. We also showed that *Pcsk9$^{-/-}$* mice exhibited increased liver stromal and tumoral apoptosis, likely because of the activation of the tumor necrosis factor–α (TNFα) pathway.

Materials and Methods

Cell Culture, Plasmids, Transfection, and Western Blot Analysis

Human embryonic kidney 293 (HEK293) cells and B16F1 cells were cultured in Dulbecco's modified Eagle's medium (Invitrogen, Burlington, Canada) and HepG2 cells in modified Eagle's medium (Invitrogen) supplemented with 10% FBS (Invitrogen). All cells were maintained at 37°C under 5% CO_2.

The cDNA of mouse or human wild-type (WT) PCSK9 and its mutant form, PCSK9^{D374Y}, were cloned into the pIRES2-EGFP vector (Clontech, Mountain View, CA), as described previously [1]. Nontargeting shRNA (NTsh) and PCSK9-targeting shRNA (PC9sh) constructs, generation of lentiviral particles, and transductions of HepG2 cells to obtain stable pools were described previously [17]. Human HEK293 and HepG2 cells and mouse B16F1 cells were transfected using Effectene (Qiagen, Toronto, Canada), Fugene HD (Roche, Laval, Canada), and Lipofectamine 2000 (Invitrogen) reagents, respectively. Stable B16F1 and HepG2 cells overexpressing either WT or PCSK9^{D374Y} were obtained upon puromycin selection.

HEK293 cells were transfected with the vector pIRES2-EGFP empty or encoding V5-tagged PCSK9 or PCSK9^{D374Y}, washed at 24 hours post-transfection, and then incubated with serum-free medium for another 24 hours. Media were then collected or transferred onto B16F1 or HepG2 cells for 12 hours. Media and cell lysate proteins were separated by 8% sodium dodecyl sulfate–polyacrylamide gel electro-

phoresis, blotted onto polyvinylidene difluoride (PVDF) membranes, and incubated with a polyclonal human PCSK9 (1:2000) [7], human or mouse LDLR (1:1000; R&D Systems, Toronto, Canada), β-actin (1:5000; Sigma, Toronto, Canada), or HRP-conjugated V5 (1:10,000; Sigma) antibodies (Abs).

RNA Isolation, Quantitative Polymerase Chain Reaction, and Quantitative Polymerase Chain Reaction Array

Liver samples were dissected from the right medial lobe. For metastatic livers, the absence of tumor contamination in the adjacent normal tissue samples (stroma) was verified by quantitative polymerase chain reaction (qPCR) analysis of transcripts for tyrosinase, an abundant enzyme implicated in melanin synthesis in B16-derived tumors (Figure W1). All cell and tissue samples were submitted to RNA extraction using TRIzol reagent (Invitrogen). cDNA were then prepared as described previously [18]. All qPCRs were carried out in a final volume of 10 μl using the SYBER Green Supermaster (Quanta Biosciences, Gaithersburg, MD) following the manufacturer's protocol. Liver WT and *Pcsk9$^{-/-}$* stromal cDNA were also submitted to a mouse apoptosis qPCR array (SuperArray, Frederick, MD) according to the manufacturer's protocol. Specific primers were used for the amplification of the following cDNAs: furin [18], PCSK9 [11], 3-hydroxy-3-methylglutaryl coenzyme A (HMG-CoA) reductase (forward: 5′-GTACGGAGAAAGCACTGCTGAA; reverse: 5′-TGACTGCCAG-AATCTGCATGTC), LDLR (forward: 5′-GTATGAGGTTCCTG-TCCATC; reverse: 5′-CCTCTGTGGTCTTCTGGTAG), TNFα (forward: 5′-CCAGAACTCCAGGCGGTGCC; reverse: 5′-CTGAT-GAGAGGGGAGGCCATTTGGGA), TNFα receptor 1 (TNFR1; forward: 5′-CCACCCGCAACGTCCTGACA; reverse: 5′-AGGCA-CGCCATCCACCACAG), B-cell lymphoma 2 (Bcl-2; forward: 5′-TGAACCGGCATCTGCACACCTG; reverse: 5′-AAACAGAG-GTCGCATGCTGGGG), and TNF receptor–associated factor 2 (TRAF2; forward: 5′-TGCCCGCAGAGAGGTGGAGAG; reverse: 5′-CCTTCTCGCTGAGGCGGACC). Simultaneously, cDNA for TATAA-box binding protein (TBP) were amplified for normalization (forward: 5′-CCTAGTGGAGGTGCCTTGGA; reverse: 5′-GGTTGCCACCTGAAGTCACA).

Animals and Experimental Metastasis Assay

Apc$^{Min/+}$ mice were obtained from the Jackson Laboratory (Bar Harbor, ME) [19]. Generation of *Pcsk9$^{-/-}$* mice that lack the proximal promoter and first exon of the *Pcsk9* gene was described previously [11], as well as that of mice lacking LDLR [20] or both LDLR and PCSK9 [15]. All mice were on the C57BL/6J background. The following procedures were approved by the Animal Care Committee of the Institut de Recherches Cliniques de Montreal. Six- to eight-week-old female mice were anesthetized with 2% isoflurane inhalation. B16F1 cells were suspended in phosphate-buffered saline (PBS; 10^5 cells/100 μl) and injected directly into spleen, and mice were sacrificed 12 days later. Mice were fed either a chow diet (2018 Teklad Global) or an HCD (TD.08464 Harlan Teklad) for 14 or 26 days before sacrifice day. Livers were then removed to be photographed. Tumor and liver areas were quantified by image software Northern Eclipse, and tumor density was calculated as the ratio of tumor area and total liver area.

B16F1 Cell Adhesion Assay

Primary hepatocytes were prepared using 10- to 12-week-old mice and the two-step collagenase perfusion method, as described

previously [21]. Hepatocytes were seeded in a 24-well plate (10^5/well) coated with 0.5 mg/ml fibronectin (Sigma-Aldrich). Only the wells in which a perfect cell monolayer was formed were used for adhesion assay. B16F1 cells (3×10^6) were labeled with 30 μCi of ^{3}H-thymidine (PerkinElmer Life Sciences, Toronto, Canada) for 24 hours. Cells were then trypsinized, washed with PBS, and suspended in 10 ml of Dulbecco's modified Eagle's medium containing 10% FBS or 10% lipoprotein-deficient serum (LPDS; Biomedical Technologies, Stoughton, MA). ^{3}H-labeled B16F1 cells (10^4 cells in 100 μl) were then added on hepatocyte monolayers, which were pre-incubated for 3 hours with FBS- or LPDS-containing media. After 1-hour adhesion, media were removed. Cells were washed and incubated with cold 10% TCA for 30 minutes, lysed in a 0.5 M NaOH/0.1% sodium dodecyl sulfate solution, and finally submitted to ^{3}H radioactivity counting.

In Vitro Cell Growth

Cells (10^4/well) were distributed in 96-well plates and subjected to 3-(4,5-dimethylthiazol-2-yl)-5-(3-carboxymethoxyphenyl)-2-(4-sulfophenyl)-2H-tetrazolium (MTS) cell proliferation assay (Promega, Madison, WI) at multiple time points. Optical absorption was read at 490 nm using a Vmax microplate reader (Molecular Devices, Sunnyvale, CA).

Apoptosis Assay

B16F1 and HepG2 cells were grown either in the absence or presence of 1 μM staurosporine (Sigma) for 12 hours. Cells were collected in reaction buffer [20 mM PIPES (pH 7.2), 100 mM NaCl, 1 mM EDTA, 0.1% CHAPS, and 10% sucrose]. Liver, hepatic tumors, and adjacent stromal tissues were dissected and homogenized (Polytron and Brinkmann Instruments, Mississauga, Canada) in reaction buffer. Cell lysis was completed by two cycles of 10 minutes freezing and thawing. Caspase-3 activity was then measured at 37°C in 80 μg of proteins using 30 μg of the caspase-3 fluorogenic substrate, acetyl-Asp-Glu-Val-Asp-7-amido-4-methylcoumarin (Calbiochem, Mississauga, Canada). The fluorescence generated by free amido-4-methylcoumarin was detected with a SpectraMAX GEMINI EM microplate spectrofluorometer (Molecular Devices; excitation, 380 nm; emission, 460 nm), and caspase-3 activity was expressed as the released relative fluoresce units per minute.

Apoptosis in liver paraffin sections was assessed using In Situ Cell Death Detection Kit, POD according to the manufacturer's instructions (Roche).

Plasma Measurement

Plasma TC was measured using the Infinity Kit (Thermo Scientific, Ottawa, Canada). Specific ELISA kits were used to measure mouse plasma PCSK9 (CircuLex, Toronto, Canada) and TNFα (Cell Signaling Technology, Pickering, Canada), according to the manufacturer's recommendations.

Results

### PCSK9 Expression Is Higher in Intestinal Tumors than in Adjacent Normal Tissues

To probe the possible involvement of PCSK9 in cancer development, we looked at its expression in various cancers reported in the ONCOMINE database (http://www.oncomine.org). PCSK9 expression was upregulated by 1.2- to 2.8-fold in all cancer types assessed (Figure W2), except in the steroid-dependent breast and prostate carcinomas, where PCSK9 was downregulated by 40% to 50%. We completed these data with the analysis of tumors in intestine, one of the major sites of PCSK9 expression [1]. At 4 months of age, the $Apc^{Min/+}$ mice, which constitute a colorectal cancer model, spontaneously develop along their small intestine about one tumor per centimeter [18,19]. A representative hematoxylin and eosin–stained tumor section is shown in Figure 1. qPCR analysis of $Apc^{Min/+}$ tumors and their adjacent normal tissues demonstrated that PCSK9 mRNA was 3.1-fold higher in tumors (Figure 1). This up-regulation was likely due to the transcriptional activation of the cholesterogenic pathway by the sterol response element binding protein 2, as LDLR and HMG-CoA reductase mRNA levels were also increased (two-fold). Thus, PCSK9 was upregulated in intestinal tumors as in most cancers.

Development of Hepatic Tumors Is Reduced in Pcsk9$^{-/-}$ Mice

The liver is the major site of PCSK9 expression with ~10-fold higher levels of mRNA than in colon and intestine [1]. To investigate the in vivo role of PCSK9 in hepatic cancer development, we
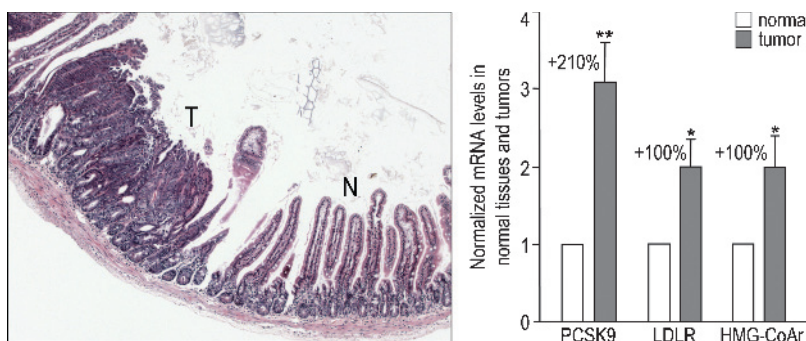
Figure 1. PCSK9 is upregulated in intestinal tumors. An $Apc^{min/+}$ mouse small intestine section stained with hematoxylin and eosin shows the structure of an intestinal tumor (T) and its adjacent normal tissue (N). Expression of PCSK9, LDLR, and HMG-CoA reductase was assessed by qPCR in 18 couples of tumors and their adjacent normal tissues collected from three $Apc^{min/+}$ mice of 4 months of age. mRNA levels in tumors were normalized to that of their respective adjacent stromal tissues, which was set to 1. Error bars represent SEM. *$P < .05$; **$P < .01$ (Student's t test).
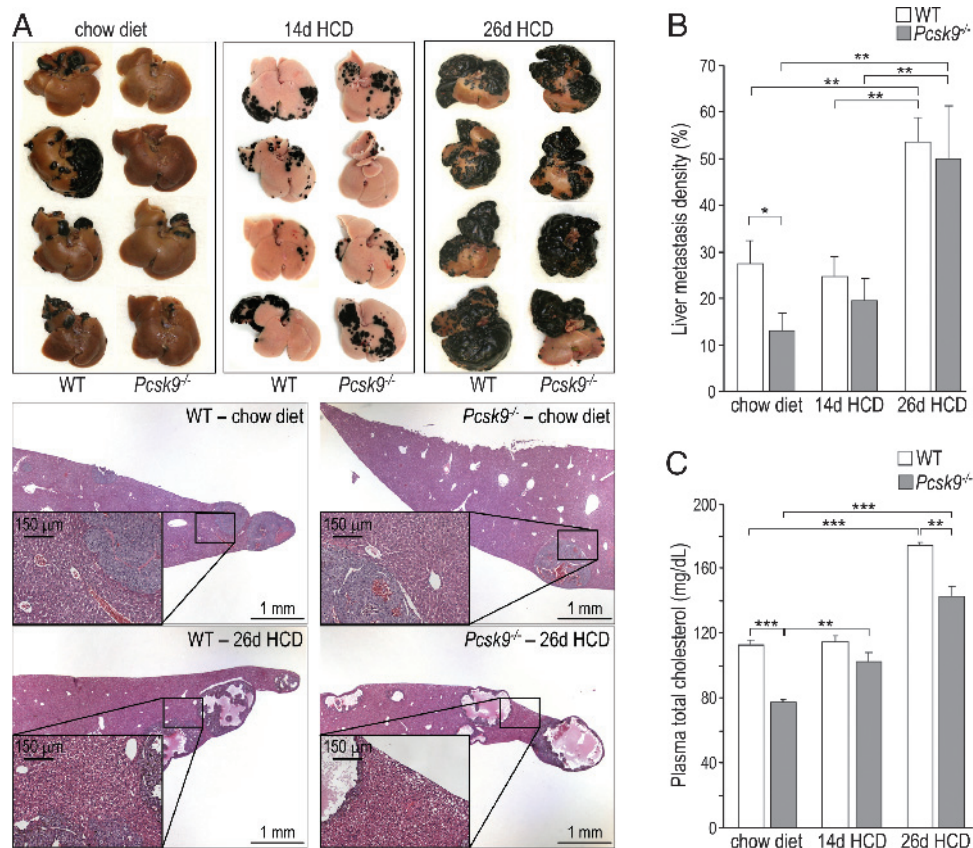
Figure 2. The loss of PCSK9 decreases hepatic metastasis in a cholesterol-dependent manner. (A) Mice were fed a chow diet or an HCD for 14 or 26 days before euthanasia and were injected with B16F1 cells 12 days before euthanasia. Livers were dissected and representative livers and liver sections are shown. Insets emphasize the accumulation of lipid droplets in the livers of mice fed an HCD for 26 days. (B) Tumor density (area of tumors/total area of liver) was evaluated in 12 to 18 mice per genotype and per condition. (C) Total cholesterol levels were measured in plasma collected on day of sacrifice. Error bars represent SEM. $*P < .05$, $**P < .01$, $***P < .001$ (Student's t test).

used a metastasis model, in which B16F1 mouse melanoma cells are injected into the spleen of C57BL/6 mice. Metastases were formed on the surface of the liver and were easily identified after 12 days because of the black melanin pigment they synthesize (Figure 2A). When 200,000 cells were injected into WT and $Pcsk9^{-/-}$ mice fed a regular chow diet, $Pcsk9^{-/-}$ mice harbored two-fold less hepatic melanoma foci than WT mice (Figure 2, A and B). To assess whether the protective effect of PCSK9 deficiency was due to its associated hypocholesterolemia (TC = 77 mg/dl *versus* 112 mg/dl for WT mice; Figure 2C) [11,22], we fed mice an HCD (0.4% cholesterol) for 14 days before euthanasia. Although this diet did not affect TC levels in WT mice, it brought $Pcsk9^{-/-}$ mice TC to 102 mg/dl, similar to 114 mg/dl in WT mice (Figure 2C). In parallel to TC levels, tumor density rose in $Pcsk9^{-/-}$ mice from 13% on a chow diet to 20% on an HCD but did not change in WT mice (27% *versus* 25%; Figure 2, A and B). When mice were fed an HCD for 26 days before euthanasia, TC levels were increased by 1.5- and 1.8-fold, and tumor density rose by ~2- and ~4-fold, in WT and $Pcsk9^{-/-}$ mice, respectively (Figure 2). In addition, mice fed a 26-day HCD exhibited tumors with a very high degree of necrosis.

The loss of statistical significance between the WT and $Pcsk9^{-/-}$ tumor densities when mice were fed an HCD indicates that the protective effect of PCSK9 deficiency mainly resides in its ability to lower circulating cholesterol levels. Furthermore, our data show that

a high dietary cholesterol intake significantly enhances the development of liver metastases.

B16F1 Cells Do Not Express PCSK9 and Their LDLR Levels Are Not Sensitive to Exogenous PCSK9

To understand the underlying molecular mechanism(s) behind the protective role of PCSK9 deficiency on liver metastases development, we analyzed by qPCR the mRNA expression of PCSK9 and other members of the PC family in B16F1 cells (Figures 3A and W3). Importantly, although PCSK9 expression was abundant in the human hepatocellular carcinoma HepG2 cells, it was extremely low in B16F1 cells and undetectable in B16F1 cell–derived hepatic tumors collected 12 days post-injection (Figure 3A). This suggests that the higher metastasis observed in WT mice is due to liver PCSK9 that modulates the host microenvironment, rather than to PCSK9 from B16F1 cells. Thus, B16F1 tumor cells constitute a good model to study the exclusive impact of host PCSK9 on metastasis.

To mimic the *in vivo* paracrine/endocrine influence of host PCSK9, we incubated B16F1 cells overnight with media from HEK293 cells expressing V5-tagged mouse PCSK9, human PCSK9, or its most potent gain-of-function mutant PCSK9[D374Y] [23,24] and analyzed PCSK9-enhanced LDLR degradation by Western blot analysis. Surprisingly, none of the three PCSK9 forms were able to degrade the LDLR in B16F1 cells. In contrast, the same media incubated with
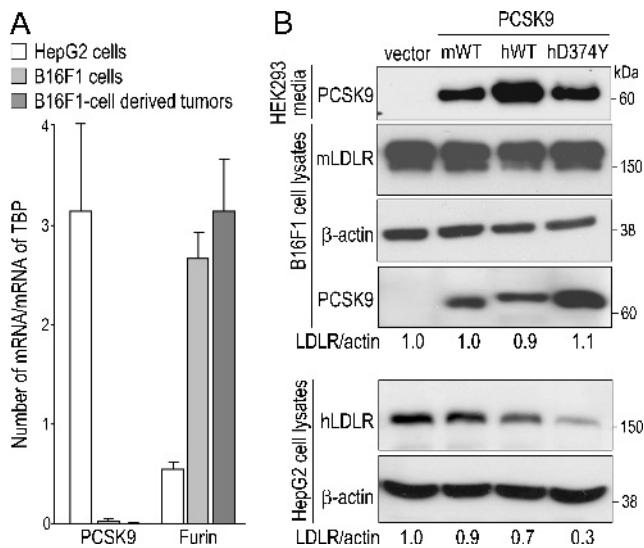
Figure 3. B16F1 cells do not express PCSK9 and their LDLR is insensitive to exogenous PCSK9. (A) PCSK9 expression was quantified by qPCR in HepG2 cells, B16F1 cells, and B16F1 cell–derived liver tumors ($n = 3$ for each). As a control, expression of the ubiquitous furin was also quantified. Error bars represent SEM. (B) Media of HEK293 cells that express the empty pIRES2-EGFP vector, mouse (mWT) or human (hWT) WT PCSK9, or human gain-of-function PCSK9[D374Y] (hD347Y), all containing a C-terminal V5 tag, were collected and transferred onto B16F1 or HepG2 cells for 12 hours. HEK293 cell media and B16F1 and HepG2 cell lysates were analyzed by Western blot analysis using a V5 Ab to reveal PCSK9 and mouse or human LDLR and β-actin Abs. Band intensities were quantified by ImageJ software and LDLR intensities were first normalized to that of β-actin (LDLR/act). Ratios were then normalized to that of the empty vector that was set to 1. A representative experiment of three is shown.

HepG2 cells can trigger LDLR degradation (Figure 3). Although exogenous PCSK9 did not affect LDLR levels, it likely bound the cell surface LDLR of B16F1 cells, as V5-immunoreactive species were detected in cell lysates, especially with PCSK9[D374Y] (Figure 3B), known to exhibit a >10-fold better binding to the LDLR [24].

Metastasis is a complex multistep process including cell extravasation from the primary tumor, intravasation and adhesion in distant organs, and proliferation to form secondary tumors [25]. In our experimental model, the final metastatic volume was shown to depend on tumor cell implantation and focal growth of metastases [26]. We thus decided to focus on the function of PCSK9 in cancer cell adhesion and proliferation.

B16F1 Cell Adhesion to Primary Hepatocytes Increases in the Absence of PCSK9

The role of PCSK9 in cell adhesion was assessed by measuring the attachment of B16F1 cells to primary hepatocytes (Figure 4). B16F1 cells were radioactively labeled by ^{3}H-thymidine incorporation and then added directly onto a monolayer of mouse primary hepatocytes. After 1-hour incubation in a cholesterol-rich (10% FBS) or cholesterol-deficient (10% LPDS) medium, cells were washed and lysed, and the radioactivity was counted. In 10% FBS, 41% more B16F1 cells adhered onto *Pcsk9*^{−/−} *versus* WT hepatocytes. This different capacity of adhesion is probably caused by a cell surface protein other than LDLR, as the same adhesion difference was observed

between *Ldlr*^{−/−} and *Ldlr*^{−/−}*Pcsk9*^{−/−} (dKO) hepatocytes. In contrast, B16F1 adhesion was insensitive to the genotype of hepatocytes in LPDS medium (Figure 4).

Because *Pcsk9*^{−/−} mice developed less metastasis than WT mice, it was surprising to observe that *Pcsk9*^{−/−} primary hepatocytes bound more B16F1 cells than WT hepatocytes in FBS media. This suggests that, *in vivo*, hypocholesterolemia blunts the adhesion potential of B16F1 cells to liver and reduces metastasis through a different mechanism than a change in adhesion.

PCSK9 Does Not Modulate the Growth and Apoptosis of B16F1 Cells but Affects Those of Liver Cells

We then examined the impact of PCSK9 on B16F1 cell proliferation. We first incubated B16F1 cells with or without 5 μg/ml of purified human PCSK9 [27] and measured cell growth using an MTS assay. Similar growth curves were obtained (Figure 5A), indicating that host PCSK9 should not affect B16F1 cell proliferation *in vivo*. To further challenge B16F1 cell growth, we grew cells stably expressing an empty vector (pIR), human PCSK9, or its gain-of-function mutant PCSK9[D374Y] in 10% FBS or 10% LPDS medium (Figure 5B). Cell proliferation was drastically reduced in the lipoprotein-deficient medium, indicating that B16F1 cell growth strongly depends on cholesterol. However, growth curves were not affected by PCSK9 overexpression, suggesting that B16F1 cell proliferation is not affected *in vivo* by PCSK9. Finally, as a control, we examined the growth of HepG2 cells whose LDLR levels are sensitive to exogenous PCSK9 (Figure 3B). HepG2 cells that stably express human PCSK9, NTsh, or antisense PC9sh [17] were grown in 10% FBS media (Figure 5C). Although higher PCSK9 levels did not affect growth, as observed for B16F1 cells, knocking down PCSK9 significantly reduced HepG2 cell growth.

The slower growth of HepG2 cells lacking PCSK9 may be due to increased cell death. Accordingly, cellular apoptosis was estimated by measuring caspase-3 enzymatic activity at basal levels and in the presence of 1 μM staurosporine, an apoptosis inducer. HepG2 cells lacking PCSK9 (PC9sh) exhibited 170% to 200% higher caspase-3
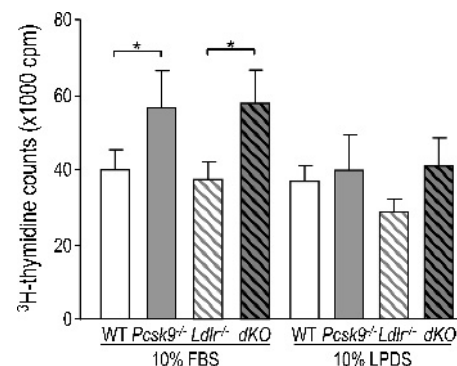
Figure 4. The adhesion of B16F1 cells to primary hepatocytes is regulated by PCSK9 and cholesterol. B16F1 cells were incubated with ^{3}H-thymidine for 24 hours and then added onto WT, *Pcsk9*^{−/−}, *Ldlr*^{−/−}, and *Ldlr*^{−/−}*Pcsk9*^{−/−} primary hepatocytes, which were preincubated in media containing either 10% FBS or 10% LPDS for 3 hours. After 1 hour of incubation, unadhered B16F1 cells were washed out, the remaining cells were lysed, and radioactivity in the total lysates was counted. The error bars indicate SEM of four independent experiments. *$P < .05$; (Student's t test).
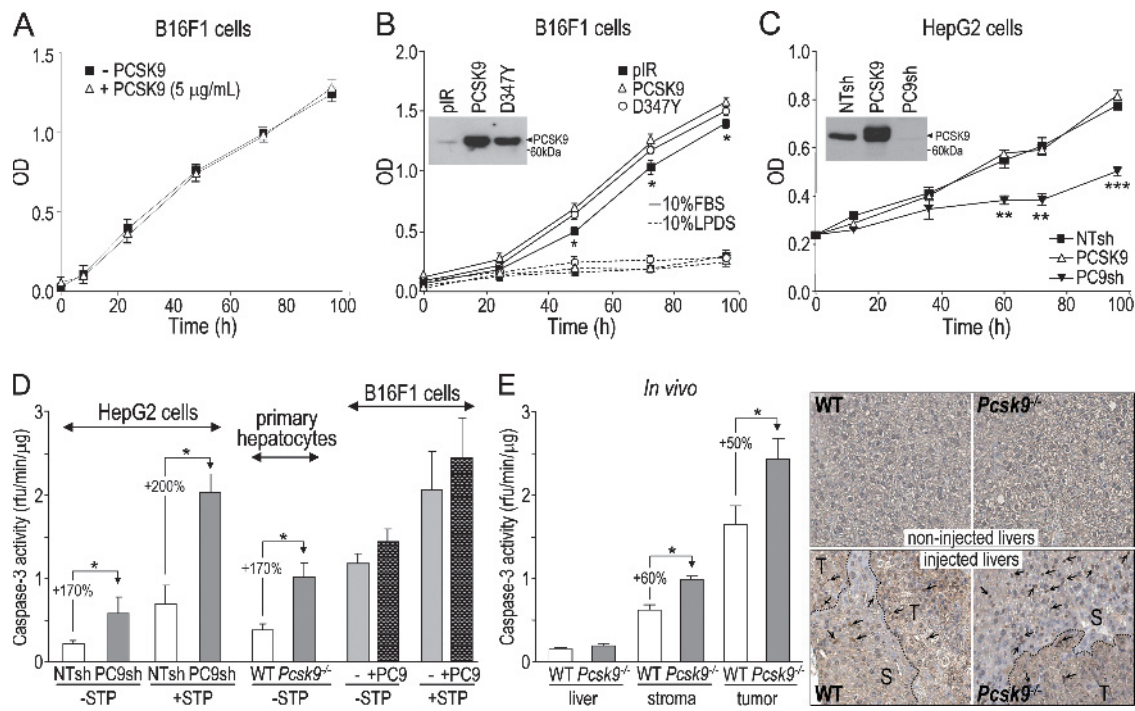
Figure 5. PCSK9 affects cell proliferation and apoptosis of hepatic cells but not those of B16F1 cells. (A) Proliferation of B16F1 cells incubated with or without 5 μg/ml of purified PCSK9, and grown in media containing 10% FBS, was measured using an MTS assay. (B) B16F1 cells stably expressing the empty pIRES2-EGFP vector (pIR), V5-tagged human PCSK9 (PCSK9), or its variant PCSK9^{D374Y} (D347Y) were grown in media containing 10% FBS or 10% LPDS and their proliferation was measured. PCSK9 expression in these cell lines was assessed by Western blot analysis of serum-free media using a V5 Ab (inset). (C) HepG2 cells stably expressing NTsh, PC9sh, or human PCSK9 were grown in media containing 10% FBS and their proliferation was measured. PCSK9 expression and efficiency of PCSK9 knockdown in these cell lines were assessed by Western blot analysis of serum-free media using a V5 Ab (inset). (D) Caspase-3 activity was measured in HepG2 cells stably expressing NTsh and PC9sh, WT and $Pcsk9^{-/-}$ primary hepatocytes, and B16F1 cells pre-incubated with or without 5 μg/ml of purified PCSK9 for 24 hours, either in the absence or presence of 1 μM staurosporine. (E) Caspase-3 activity was assessed in non-injected liver extracts and in liver stroma and tumor extracts obtained from mice 12 days post–B16F1 cell injection. Liver sections from both non-injected and B16F1 cell–injected WT and $Pcsk9^{-/-}$ mice were submitted to a TUNEL assay. Arrows point at labeled apoptotic nuclei and dashed lines separate tumoral (T) and stromal (S) areas. The error bars indicate SEM of three independent experiments (A–D) or data for six mice per genotype (E). *$P < .05$, **$P < .01$, ***$P < .001$ (Student's t test).

activity *versus* control HepG2 cells (NTsh; Figure 5D). Similarly, caspase-3 activity in $Pcsk9^{-/-}$ primary hepatocytes was 170% higher than in WT ones (Figure 5D). In contrast, B16F1 cells pre-incubated with or without 5 μg/ml of purified PCSK9 for 24 hours exhibited similar caspase-3 activity, in the absence or presence of staurosporine (Figure 5D). Thus, *in vitro*, only the absence of PCSK9 had an effect on HepG2 cell proliferation, likely through increased apoptosis, whereas PCSK9 had no major effect on B16F1 cell proliferation or apoptosis.

In vivo, basal caspase-3 activities in WT and $Pcsk9^{-/-}$ livers were similar. However, like in HepG2 cells, injected livers lacking PCSK9 exhibited 50% higher caspase-3 activities, both in B16F1 cell–derived liver tumors and their adjacent stromal tissues (Figure 5E). This was confirmed by terminal deoxynucleotidyl transferase dUTP nick end labeling (TUNEL) assay on corresponding liver sections. In tumoral regions, the labeling was highly concentrated in the center of the tumor, making any quantification of the number of cells in apoptosis difficult. However, $Pcsk9^{-/-}$ stromal regions exhibited a stronger labeling than WT ones, whereas non-injected liver sections only showed a background signal.

In summary, these data suggest that the absence of PCSK9 causes higher apoptosis in hepatic stromal and tumoral cells. The increased apoptosis observed in tumors is probably indirect, as incubation of B16F1 cells with PCSK9 failed to change their caspase-3 activity.

TNFα Pathway Is Affected in Pcsk9$^{-/-}$ Liver

To identify the underlying molecular pathway that promotes apoptosis in the absence of PCSK9, we performed a qPCR array analysis of 84 key genes involved in apoptosis on WT and $Pcsk9^{-/-}$ liver stroma tissues that were collected 12 days after B16F1 cell injection. A set of genes was dysregulated in $Pcsk9^{-/-}$ mice (Table W1), and the expression of selected genes was validated by qPCR in non-injected livers, hepatic tumors, and stroma samples (Figure 6). The most upregulated gene encodes TNFα, an inflammatory cytokine. qPCR analysis confirmed that TNFα expression was 50% higher in $Pcsk9^{-/-}$ stromal samples than in WT samples (Figure 6). $Pcsk9^{-/-}$ *versus* WT non-injected livers also showed a trend for higher TNFα expression, but TNFα expression was similar in WT and $Pcsk9^{-/-}$ tumors.

To better assess the role of PCSK9 in TNFα gene regulation, we took advantage of our transgenic mice, *Tg(Apoe-PCSK9)*, in which the apoE promoter drives the expression of PCSK9 essentially in the liver and macrophages [11]. First, *Tg(Apoe-PCSK9)* livers expressed 38% less TNFα than $Pcsk9^{-/-}$ livers (Figure W4). Second, naïve peritoneal macrophages express >200-fold higher levels of TNFα than liver. When isolated from $Pcsk9^{-/-}$ mice, their TNFα expression was 70% and 130% higher than in macrophages isolated from WT and *Tg(Apoe-PCSK9)*, respectively (Figure W4). Thus, these data confirm

the existence of an inverse correlation between PCSK9 and TNFα expression levels.

The expression of TNFR1 (gene *Tnfsfr1a*) was similar in WT and *Pcsk9*$^{-/-}$ intact livers. However, injection of B16F1 cells significantly induced TNFR1 expression by 50% and 110% in WT and *Pcsk9*$^{-/-}$ liver stroma tissues, respectively, resulting in a 40% higher expression of TNFR1 in the *Pcsk9*$^{-/-}$ stroma (Figure 6). Like TNFα, TNFR1 is similarly expressed in liver tumors developed in WT or *Pcsk9*$^{-/-}$ mice. Thus, the 40% higher expression of TNFR1 in the *Pcsk9*$^{-/-}$ stroma should potentiate TNFα signaling in this tissue.

The binding of TNFα to TNFR1 can simultaneously elicit apoptotic and nuclear factor κB (NF-κB)–mediated cell survival signals [28]. NF-κB negatively regulates apoptosis by inducing the expression of anti-apoptotic factors [29], including Bcl-2 [30] and the TRAF2, whose deficiency was shown to increase cell sensitivity to TNFα-induced apoptosis [31,32] (Figure 6, *lower right panel*). Expression of both TRAF2 and Bcl-2 was 30% lower in *Pcsk9*$^{-/-}$ liver stroma than in WT ones (Figure 6). In addition, Bcl-2 was down-regulated by 20% in *Pcsk9*$^{-/-}$ tumors compared to WT ones. This suggests that the absence of PCSK9 reduces the NF-κB survival response and thus further increases cell susceptibility to apoptosis.

We then verified whether TNFα up-regulation depended on the LDLR. Mice lacking the LDLR (*Ldlr*$^{-/-}$) or both the LDLR and PCSK9 (*Ldlr*$^{-/-}$*Pcsk9*$^{-/-}$, dKO) [11] and that exhibit similar high plasma TC levels were analyzed before or after B16F1 cell injection. The higher TNFα expression associated with the lack of PCSK9 was conserved in the LDLR-deficient background. TNFα mRNA levels were 90% higher in stroma (Figure 6, *lower middle panel*), showing that TNFα up-regulation does not depend on the LDLR.

In summary, these data indicate that, in an LDLR-independent manner, PCSK9 deficiency leads to a stronger TNFα pro-apoptotic signaling in liver stroma. In addition, *Pcsk9*$^{-/-}$ stroma and tumor exhibited a reduced NF-κB pro-survival response that likely reinforces apoptosis in these tissues.

Circulating TNFα and PCSK9 Are Co-regulated in the Course of Metastasis Progression

To confirm that the up-regulation of TNFα expression led to a higher TNFα secretion, we measured the plasma levels of TNFα by ELISA before injection and 2 and 12 days post–B16F1 cell injection. At all times, TNFα levels were about two-fold higher in *Pcsk9*$^{-/-}$ plasma than in WT plasma (Figure 7A). In addition, in both genotypes,
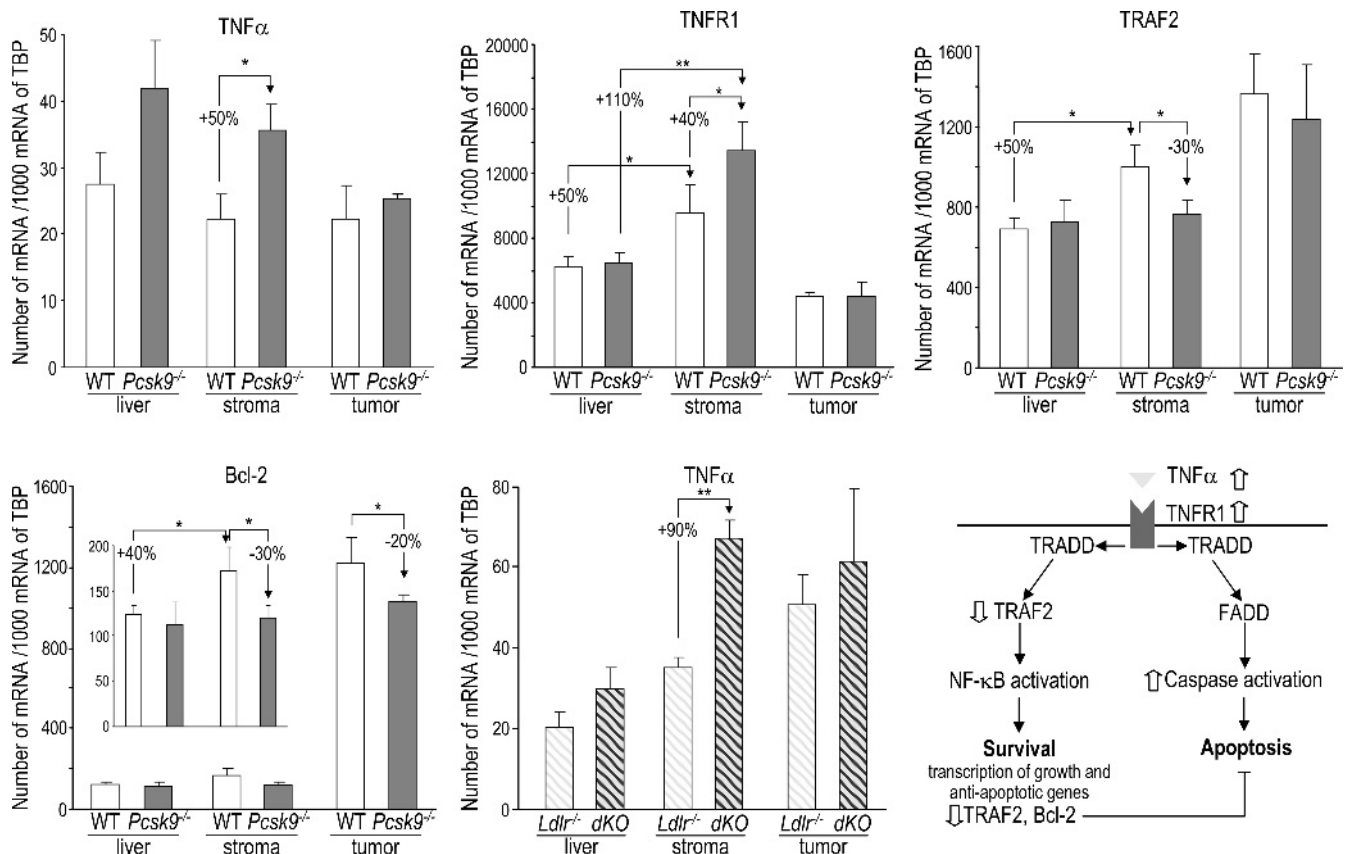
Figure 6. TNFα pathway is altered in *Pcsk9*$^{-/-}$ mice. Expression of TNFα, TNFR1, TRAF2, and Bcl-2 was analyzed by qPCR in non-injected livers (*n* = 9/genotype) and in liver stroma and tumors (*n* = 5–7/genotype) collected from mice 12 days post-injection. TNFα expression was also assessed in non-injected livers (*n* = 12/genotype) and in liver stroma and tumors (*n* = 5/genotype) collected from *Ldlr*$^{-/-}$ and *Ldlr*$^{-/-}$*Pcsk9*$^{-/-}$ (dKO) mice (hatched bars). Error bars indicate SEM. *P < .05; **P < .01 (Student's *t* test). In the lower right panel, a scheme of the TNFα signaling pathway is shown. Binding of TNFα to TNFR1 triggers intracellular recruitment of TNF receptor–associated death domain to TNFR1, which provides an assembly platform for TRAF2 and Fas-associated protein with a death domain (FADD). The binding of TRAF2 leads to NF-κB activation that induces the transcription of survival and anti-apoptotic proteins, including Bcl-2 and TRAF2. The binding of FADD leads to caspase activation and apoptosis. The events regulated by the absence of PCSK9 are indicated by open arrows.
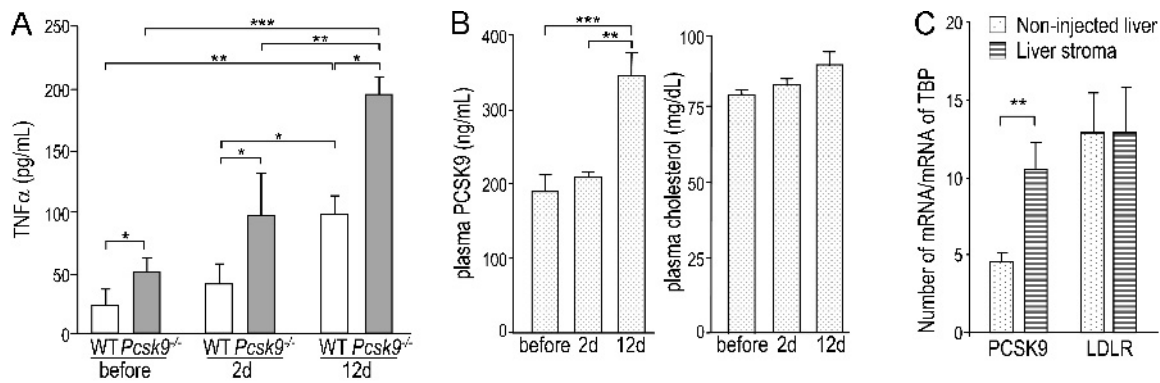
Figure 7. Plasma TNFα and PCSK9 are upregulated along metastasis formation. (A) TNFα was measured before injection and 2 and 12 days post-injection in the plasma of WT and $Pcsk9^{-/-}$ mice (n = 12/genotype). (B) Circulating PCSK9 and plasma TC were measured before injection and 2 and 12 days post-injection in WT mice (n = 12). (C) PCSK9 and LDLR expression levels were measured by qPCR in non-injected livers and in B16F1 cell–injected livers (stroma) from WT mice (n = 5). The data are represented by the means ± SEM. *P < .05; **P < .01; ***P < .001 (Student's t test).

TNFα levels increased with time, reaching four-fold higher levels at 12 days post-injection. In the same WT plasma samples, circulating PCSK9 increased by 1.8-fold at 12 days post-injection, whereas cholesterol levels were unaffected (Figure 7B). In agreement, we confirmed by qPCR that PCSK9 transcripts were 2.3-fold higher in stroma than in non-injected livers, whereas LDLR transcripts were unchanged (Figure 7C). This suggests that the increases in TNFα and PCSK9 were independent of cholesterol [33].

Discussion

In this study, we investigated the role of PCSK9 in liver metastasis formation, following B16F1 cells injection in the spleen of WT and $Pcsk9^{-/-}$ mice. Because B16F1 cells and their derived tumors do not express PCSK9 and exhibit LDLR levels that are insensitive to exogenous PCSK9, we exclusively examined the role of the host PCSK9 in metastasis development. First, we showed that PCSK9 enhances liver metastasis development through its role in maintaining high circulating cholesterol levels, as 1) an HCD that brought back the low cholesterol levels of $Pcsk9^{-/-}$ mice to WT levels resulted in increased metastasis in $Pcsk9^{-/-}$ mice and 2) an extended HCD enhanced liver metastasis development in both genotypes. Second, we showed that PCSK9 protects HepG2 cells, primary hepatocytes, and liver stroma and metastases against apoptosis, at least in part by maintaining low levels of TNFα expression in an LDLR/cholesterol-independent manner.

Tumor development depends on the reciprocal interaction of the tumor with its microenvironment. Locally activated stromal cells modify the proliferative and invasive behavior of cancer cells [34]. Diminished liver metastases in $Pcsk9^{-/-}$ mice revealed that the lack of PCSK9 generates a less permissive environment for tumor expansion. First, tumor cell proliferation may be indirectly limited in $Pcsk9^{-/-}$ mice, as the proliferation of B16F1 cells in $vitro$ strongly depends on cholesterol. Second, increased apoptosis in liver stroma and metastases may contribute to lower metastasis in $Pcsk9^{-/-}$ mice. However, the relative contributions of lower proliferation $versus$ higher apoptosis to the $Pcsk9^{-/-}$ protective phenotype remain to be determined.

PCSK9 was originally named "neural apoptosis-regulated candidate-1" because of its up-regulation upon induction of apoptosis by serum withdrawal [35]. Since then, the implication of PCSK9 in apoptosis has been frequently evoked. In hepatic cells and tissues, PCSK9 seems to be anti-apoptotic. A microarray study showed that overexpression of the gain-of-function PCSK9^{D347Y} downregulates some pro-apoptotic genes in HepG2 cells [10]. Additionally, the lack of PCSK9 enhances apoptosis during liver regeneration [11]. In contrast, an in $vitro$ study revealed that PCSK9 has a pro-apoptotic effect in primary cultures of cerebellar granular neurons through its ability to degrade the apolipoprotein receptor 2 [36]. However, unlike neuronal primary cultures, liver expresses very low levels of this receptor. Thus, the present study constitutes the first in $vivo$ evidence that PCSK9 has an anti-apoptotic effect in the mouse liver.

What are the underlying mechanisms of the anti-apoptotic properties of PCSK9? Surprisingly, even though PCSK9 had no effect on B16F1 cell apoptosis, B16F1 cell–derived tumors exhibited higher caspase-3 activities, suggesting apoptosis was initiated by a stromal apoptotic factor. TNFα is a good candidate. It was upregulated in liver stroma but not in tumors. It was also two-fold higher in $Pcsk9^{-/-}$ plasma. Furthermore, TNFα is a potent anti-cancer agent used to treat advanced soft-tissue sarcomas and melanoma, because of its ability to induce tumor cell apoptosis [37,38]. Although TNFα can also activate NF-κB–mediated cell survival responses, NF-κB signaling was rather reduced in $Pcsk9^{-/-}$ stroma, as lower mRNA levels of its downstream targets Bcl-2 and TRAF2 were measured. Finally, the modest, but significant, TNFα up-regulation observed was independent of 1) circulating cholesterol levels, which remained unchanged during metastasis development, or 2) LDLR, as the same TNFα increase was observed in mice lacking both PCSK9 and LDLR and exhibiting hypercholesterolemia (~300 mg/dl TC).

One of the objectives of this work was to assess the safety of PCSK9 inhibition, which may be widely used to control hypercholesterolemia. Unlike the clear association between hypercholesterolemia and elevated risk of cardiovascular diseases [4], the relation between cholesterol and cancer remains unclear. This is mainly due to the high heterogeneity of this disease. Cholesterol levels have been positively correlated with cancers of brain [39], colon [40], and prostate [41], suggesting that cholesterol-lowering drugs could be beneficial to manage the progression of these cancers. For instance, statins that inhibit cholesterol synthesis have been proven to

be effective to limit the growth and progression of prostate cancer [42,43]. In contrast, cholesterol levels have been negatively correlated with cancers of breast [39], lung [40], and liver [44,45]. However, the latter correlation is confounded by a preclinical effect, in which plasma cholesterol declines before the diagnosis of cancer [46]. Furthermore, although a negative correlation between the risk of primary liver cancer and cholesterol has been shown in humans [44,45], a mouse study demonstrated that lower plasma cholesterol levels, achieved by a cholesterol synthesis inhibitor, significantly reduced liver metastasis [47]. In agreement with the latter study, the present work that monitored liver metastasis progression, but not primary liver cancer, strongly suggests an adverse role of cholesterol. Thus, future PCSK9 inhibitors that lower LDLc [8] may also be beneficial to control hepatic metastasis progression.

The beneficial effect of PCSK9 deficiency resides 1) in its associated hypocholesterolemia that may decrease B16F1 cell growth and 2) in increased cell apoptosis, likely due to chronically elevated levels of TNFα. Even though this work was focused on melanoma, it suggests that a PCSK9 inhibitor, initially developed to treat hypercholesterolemia [8], may be useful in therapies directed against melanoma and possibly other types of cancer metastasis.

Acknowledgments

References

[1] Seidah NG, Benjannet S, Wickham L, Marcinkiewicz J, Jasmin SB, Stifani S, Basak A, Prat A, and Chretien M (2003). The secretory proprotein convertase neural apoptosis-regulated convertase 1 (NARC-1): liver regeneration and neuronal differentiation. *Proc Natl Acad Sci USA* **100**, 928–933.

[2] Abifadel M, Varret M, Rabes JP, Allard D, Ouguerram K, Devillers M, Cruaud C, Benjannet S, Wickham L, Erlich D, et al. (2003). Mutations in PCSK9 cause autosomal dominant hypercholesterolemia. *Nat Genet* **34**, 154–156.

[3] Cohen J, Pertsemlidis A, Kotowski IK, Graham R, Garcia CK, and Hobbs HH (2005). Low LDL cholesterol in individuals of African descent resulting from frequent nonsense mutations in PCSK9. *Nat Genet* **37**, 161–165.

[4] Cohen JC, Boerwinkle E, Mosley TH Jr, and Hobbs HH (2006). Sequence variations in PCSK9, low LDL, and protection against coronary heart disease. *N Engl J Med* **354**, 1264–1272.

[5] Maxwell KN, Fisher EA, and Breslow JL (2005). Overexpression of PCSK9 accelerates the degradation of the LDLR in a post-endoplasmic reticulum compartment. *Proc Natl Acad Sci USA* **102**, 2069–2074.

[6] Zhang DW, Garuti R, Tang WJ, Cohen JC, and Hobbs HH (2008). Structural requirements for PCSK9-mediated degradation of the low-density lipoprotein receptor. *Proc Natl Acad Sci USA* **105**, 13045–13050.

[7] Nassoury N, Blasiole DA, Tebon OA, Benjannet S, Hamelin J, Poupon V, McPherson PS, Attie AD, Prat A, and Seidah NG (2007). The cellular trafficking of the secretory proprotein convertase PCSK9 and its dependence on the LDLR. *Traffic* **8**, 718–732.

[8] Seidah NG and Prat A (2012). The biology and therapeutic targeting of the proprotein convertases. *Nat Rev Drug Discov* **11**, 367–383.

[9] Lan H, Pang L, Smith MM, Levitan D, Ding W, Liu L, Shan L, Shah VV, Laverty M, Arreaza G, et al. (2010). Proprotein convertase subtilisin/kexin type 9 (PCSK9) affects gene expression pathways beyond cholesterol metabolism in liver cells. *J Cell Physiol* **224**, 273–281.

[10] Ranheim T, Mattingsdal M, Lindvall JM, Holla OL, Berge KE, Kulseth MA, and Leren TP (2008). Genome-wide expression analysis of cells expressing gain of function mutant D374Y-PCSK9. *J Cell Physiol* **217**, 459–467.

[11] Zaid A, Roubtsova A, Essalmani R, Marcinkiewicz J, Chamberland A, Hamelin J, Tremblay M, Jacques H, Jin W, Davignon J, et al. (2008). Proprotein convertase subtilisin/kexin type 9 (PCSK9): hepatocyte-specific low-density lipoprotein receptor degradation and critical role in mouse liver regeneration. *Hepatology* **48**, 646–654.

[12] Mbikay M, Sirois F, Mayne J, Wang GS, Chen A, Dewpura T, Prat A, Seidah NG, Chretien M, and Scott FW (2010). PCSK9-deficient mice exhibit impaired glucose tolerance and pancreatic islet abnormalities. *FEBS Lett* **584**, 701–706.

[13] Benn M, Tybjaerg-Hansen A, Stender S, Frikke-Schmidt R, and Nordestgaard BG (2011). Low-density lipoprotein cholesterol and the risk of cancer: a Mendelian randomization study. *J Natl Cancer Inst* **103**, 508–519.

[14] Folsom AR, Peacock JM, and Boerwinkle E (2007). Sequence variation in proprotein convertase subtilisin/kexin type 9 serine protease gene, low LDL cholesterol, and cancer incidence. *Cancer Epidemiol Biomarkers Prev* **16**, 2455–2458.

[15] Roubtsova A, Munkonda MN, Awan Z, Marcinkiewicz J, Chamberland A, Lazure C, Cianflone K, Seidah NG, and Prat A (2011). Circulating proprotein convertase subtilisin/kexin 9 (PCSK9) regulates VLDLR protein and triglyceride accumulation in visceral adipose tissue. *Arterioscler Thromb Vasc Biol* **31**, 785–791.

[16] Barbera-Guillem E, Alonso-Varona A, and Vidal-Vanaclocha F (1989). Selective implantation and growth in rats and mice of experimental liver metastasis in acinar zone one. *Cancer Res* **49**, 4003–4010.

[17] Poirier S, Mayer G, Poupon V, McPherson PS, Desjardins R, Ly K, Asselin MC, Day R, Duclos FJ, Witmer M, et al. (2009). Dissection of the endogenous cellular pathways of PCSK9-induced low density lipoprotein receptor degradation: evidence for an intracellular route. *J Biol Chem* **284**, 28856–28864.

[18] Sun X, Essalmani R, Seidah NG, and Prat A (2009). The proprotein convertase PC5/6 is protective against intestinal tumorigenesis: *in vivo* mouse model. *Mol Cancer* **8**, 73–81.

[19] Su LK, Kinzler KW, Vogelstein B, Preisinger AC, Moser AR, Luongo C, Gould KA, and Dove WF (1992). Multiple intestinal neoplasia caused by a mutation in the murine homolog of the APC gene. *Science* **256**, 668–670.

[20] Ishibashi S, Brown MS, Goldstein JL, Gerard RD, Hammer RE, and Herz J (1993). Hypercholesterolemia in low density lipoprotein receptor knockout mice and its reversal by adenovirus-mediated gene delivery. *J Clin Invest* **92**, 883–893.

[21] Essalmani R, Susan-Resiga D, Chamberland A, Abifadel M, Creemers JW, Boileau C, Seidah NG, and Prat A (2011). *In vivo* evidence that furin from hepatocytes inactivates PCSK9. *J Biol Chem* **286**, 4257–4263.

[22] Rashid S, Curtis DE, Garuti R, Anderson NN, Bashmakov Y, Ho YK, Hammer RE, Moon YA, and Horton JD (2005). Decreased plasma cholesterol and hypersensitivity to statins in mice lacking *Pcsk9*. *Proc Natl Acad Sci USA* **102**, 5374–5379.

[23] Timms KM, Wagner S, Samuels ME, Forbey K, Goldfine H, Jammulapati S, Skolnick MH, Hopkins PN, Hunt SC, and Shattuck DM (2004). A mutation in PCSK9 causing autosomal-dominant hypercholesterolemia in a Utah pedigree. *Hum Genet* **114**, 349–353.

[24] Cunningham D, Danley DE, Geoghegan KF, Griffor MC, Hawkins JL, Subashi TA, Varghese AH, Ammirati MJ, Culp JS, Hoth LR, et al. (2007). Structural and biophysical studies of PCSK9 and its mutants linked to familial hypercholesterolemia. *Nat Struct Mol Biol* **14**, 413–419.

[25] Khatib AM, Siegfried G, Chretien M, Metrakos P, and Seidah NG (2002). Proprotein convertases in tumor progression and malignancy: novel targets in cancer therapy. *Am J Pathol* **160**, 1921–1935.

[26] Barbera-Guillem E, Barcelo JR, Urcelay B, Alonso-Varona AI, and Vidal-Vanaclocha F (1988). Noncorrelation between implantation and growth of tumor cells for their final metastatic efficiency. *Invasion Metastasis* **8**, 266–284.

[27] Benjannet S, Saavedra YG, Hamelin J, Asselin MC, Essalmani R, Pasquato A, Lemaire P, Duke G, Miao B, Duclos F, et al. (2010). Effects of the prosegment and pH on the activity of PCSK9: evidence for additional processing events. *J Biol Chem* **285**, 40965–40978.

[28] Heyninck K and Beyaert R (2001). Crosstalk between NF-κB-activating and apoptosis-inducing proteins of the TNF-receptor complex. *Mol Cell Biol Res Commun* **4**, 259–265.

[29] Barkett M and Gilmore TD (1999). Control of apoptosis by Rel/NF-κB transcription factors. *Oncogene* **18**, 6910–6924.

[30] Tamatani M, Che YH, Matsuzaki H, Ogawa S, Okado H, Miyake S, Mizuno T, and Tohyama M (1999). Tumor necrosis factor induces Bcl-2 and Bcl-x expression through NFκB activation in primary hippocampal neurons. *J Biol Chem* **274**, 8531–8538.

[31] Tada K, Okazaki T, Sakon S, Kobarai T, Kurosawa K, Yamaoka S, Hashimoto H, Mak TW, Yagita H, Okumura K, et al. (2001). Critical roles of TRAF2 and

TRAF5 in tumor necrosis factor-induced NF-κB activation and protection from cell death. *J Biol Chem* **276**, 36530–36534.

[32] Wang CY, Mayo MW, Korneluk RG, Goeddel DV, and Baldwin AS Jr (1998). NF-κB antiapoptosis: induction of TRAF1 and TRAF2 and c-IAP1 and c-IAP2 to suppress caspase-8 activation. *Science* **281**, 1680–1683.

[33] Dubuc G, Chamberland A, Wassef H, Davignon J, Seidah NG, Bernier L, and Prat A (2004). Statins upregulate PCSK9, the gene encoding the proprotein convertase neural apoptosis-regulated convertase-1 implicated in familial hypercholesterolemia. *Arterioscler Thromb Vasc Biol* **24**, 1454–1459.

[34] Tlsty TD and Coussens LM (2006). Tumor stroma and regulation of cancer development. *Annu Rev Pathol* **1**, 119–150.

[35] Chiang LW, Grenier JM, Ettwiller L, Jenkins LP, Ficenec D, Martin J, Jin F, DiStefano PS, and Wood A (2001). An orchestrated gene expression component of neuronal programmed cell death revealed by cDNA array analysis. *Proc Natl Acad Sci USA* **98**, 2814–2819.

[36] Kysenius K, Muggalla P, Matlik K, Arumae U, and Huttunen HJ (2012). PCSK9 regulates neuronal apoptosis by adjusting ApoER2 levels and signaling. *Cell Mol Life Sci* **69**, 1903–1916.

[37] Eggermont AM, de Wilt JH, and ten Hagen TL (2003). Current uses of isolated limb perfusion in the clinic and a model system for new strategies. *Lancet Oncol* **4**, 429–437.

[38] Alegre JF, Duarte M, Sureda GM, Bretcha BP, Dussan C, Ballester A, Crespo A, and Brugarolas MA (2012). Tumor necrosis factor α and melfalan-based hyperthermic isolated limb perfusion in locally advanced extremity soft tissue sarcomas and melanomas. *Cir Esp* **90**, 114–120.

[39] Kritchevsky SB and Kritchevsky D (1992). Serum cholesterol and cancer risk: an epidemiologic perspective. *Annu Rev Nutr* **12**, 391–416.

[40] Kitahara CM, Berrington de González A, Freedman ND, Huxley R, Mok Y, Jee SH, and Samet JM (2011). Total cholesterol and cancer risk in a large prospective study in Korea. *J Clin Oncol* **29**, 1592–1598.

[41] Platz EA, Clinton SK, and Giovannucci E (2008). Association between plasma cholesterol and prostate cancer in the PSA era. *Int J Cancer* **123**, 1693–1698.

[42] Gutt R, Tonlaar N, Kunnavakkam R, Karrison T, Weichselbaum RR, and Liauw SL (2010). Statin use and risk of prostate cancer recurrence in men treated with radiation therapy. *J Clin Oncol* **28**, 2653–2659.

[43] Murtola TJ, Syvala H, Pennanen P, Blauer M, Solakivi T, Ylikomi T, and Tammela TL (2011). Comparative effects of high and low-dose simvastatin on prostate epithelial cells: the role of LDL. *Eur J Pharmacol* **673**, 96–100.

[44] Iso H, Ikeda A, Inoue M, Sato S, and Tsugane S (2009). Serum cholesterol levels in relation to the incidence of cancer: the JPHC study cohorts. *Int J Cancer* **125**, 2679–2686.

[45] Borena W, Strohmaier S, Lukanova A, Bjorge T, Lindkvist B, Hallmans G, Edlinger M, Stocks T, Nagel G, Manjer J, et al. (2012). Metabolic risk factors and primary liver cancer in a prospective study of 578,700 adults. *Int J Cancer* **131**, 193–200.

[46] Kritchevsky SB, Wilcosky TC, Morris DL, Truong KN, and Tyroler HA (1991). Changes in plasma lipid and lipoprotein cholesterol and weight prior to the diagnosis of cancer. *Cancer Res* **51**, 3198–3203.

[47] Broitman SA, Wilkinson J, Cerda S, and Branch SK (1996). Effects of monoterpenes and mevinolin on murine colon tumor CT-26 *in vitro* and its hepatic "metastases" *in vivo*. *Adv Exp Med Biol* **401**, 111–130.
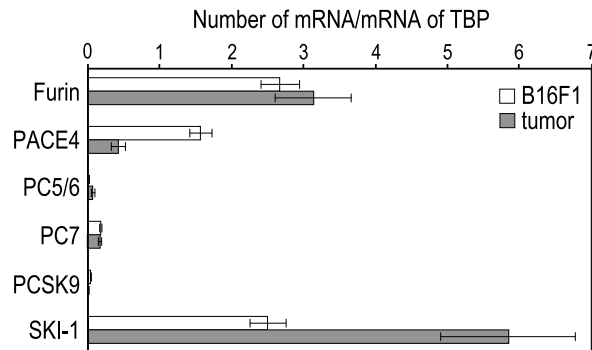
Number of tyrosinase mRNA/mRNA of TBP
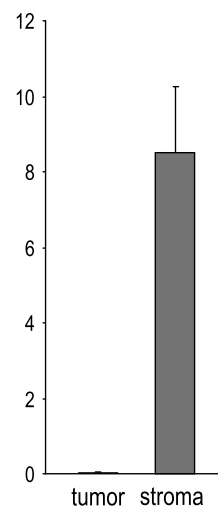
Figure W1. Tyrosinase expression in liver tumor and stroma. The absence of contamination of the liver stroma samples by tumoral cells was verified by assessing tyrosinase expression by qPCR in these samples ($n = 12$). Tyrosinase is implicated in the synthesis of the melanin pigment that is abundantly produced by tumoral cells. The primers used for the amplification of tyrosinase cDNA were given as follows: forward, 5′-CACAGGCACCTATGGCCAAAT-GAAC; reverse, 5′-CCAGTATGGAACAGTGAAGTTCTCATC. Error bars indicate SEM.
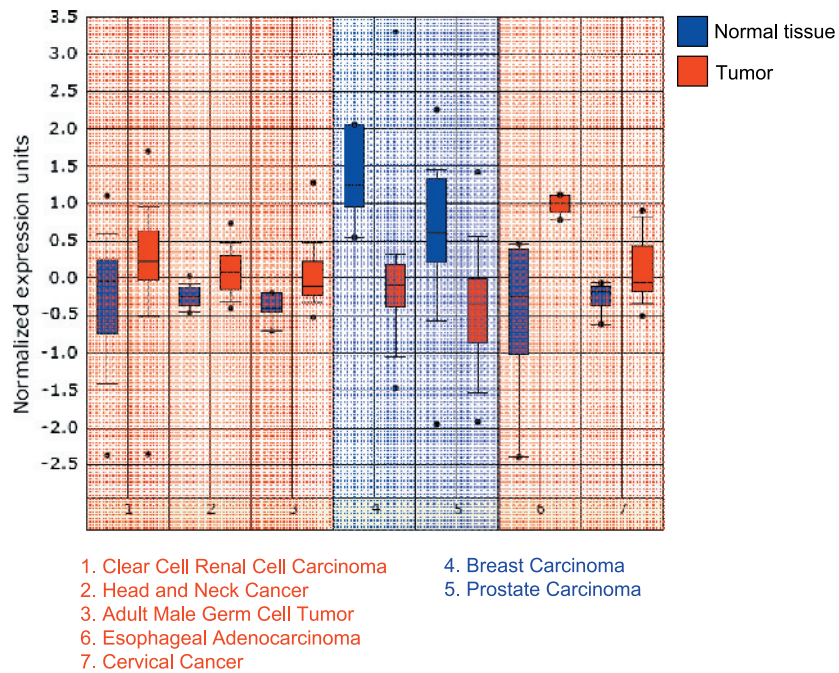
Figure W2. Expression of PCSK9 in various cancers. Data sets were retrieved from ONCOMINE (a cancer microarray database and integrated data mining platform) with a threshold of $P < .0001$. PCSK9 expression value in tumors was $\log_2$ transformed and normalized by that in the adjacent normal tissue. Cancers in which PCSK9 was upregulated or downregulated are listed in red or blue, respectively.

1. Clear Cell Renal Cell Carcinoma
2. Head and Neck Cancer
3. Adult Male Germ Cell Tumor
6. Esophageal Adenocarcinoma
7. Cervical Cancer

4. Breast Carcinoma
5. Prostate Carcinoma

Figure W3. PC expression in B16F1 cells. Mouse furin, PC5/6, PACE4, PC7, PCSK9, and SKI-1 expression were quantified by qPCR in B16F1 cells ($n = 3$) and B16F1 cell–derived liver tumors ($n = 3$). The primers used to amplify these cDNA were reported previously [18].

Table W1. Comparative Expression of 84 Key Genes Associated with Apoptosis in WT and *Pcsk9*$^{-/-}$ Liver Stroma.

Genes	GenBank	Fold Change KO/WT
Tnf	NM_013693	5.28
Bak1	NM_007523	2.27
Nme5	NM_080637	2.01
Tnfrsf1a	NM_011609	1.96
Bcl10	NM_009740	1.46
Fas	NM_007987	1.41
Dffa	NM_010044	1.40
Tnfrsf11b	NM_008764	1.35
Sphk2	NM_147325	1.35
Zc3hc1	NM_172735	1.34
Casp4	NM_007609	1.31
Fasl	NM_010177	1.31
Birc1a	NM_008670	1.31
Ripk1	NM_009068	1.30
casp2	NM_007610	1.28
Polb	NM_011130	1.27
Nol3	NM_030152	1.24
Birc2	NM_007465	1.24
Card6	XM_139295	1.20
Bnip3	NM_009760	1.13
Casp6	NM_009811	1.13
Card4	NM_172729	1.13
Dffb	NM_007859	1.12
Prdx2	NM_011563	1.09
Bad	NM_007522	1.07
Bnip3l	NM_009761	1.06
Tnfsf12	NM_011614	1.05
Tnfrsf5	NM_011611	1.05
Traf3	NM_011632	1.05
Bmip2	NM_016787	1.04
Mcl1	NM_008562	1.03
Card10	NM_130859	1.03
Fadd	NM_010175	1.01
Casp9	NM_015733	1.00
Birc4	NM_009688	0.99
Dab1	NM_010015	0.98
Apaf1	NM_009684	0.98
Dapk1	NM_029653	0.98
Bcl2l2	NM_007537	0.97
Casp8	NM_009812	0.97
Bax	NM_007527	0.96
Cflar	NM_009805	0.95
Rnf7	NM_135065	0.95
Ltbr	NM_010736	0.95
Pim2	NM_145737	0.91
Tnfrsf10b	NM_020275	0.91
Bid	NM_007544	0.89
Birc3	NM_007464	0.88
Birc1b	NM_010872	0.88
Bag1	NM_009736	0.87
Casp12	NM_009808	0.86
Api5	NM_007466	0.85
Nfkb1	NM_008689	0.83
Bag3	NM_013863	0.81
Bok	NM_016778	0.81
Akt1	NM_009652	0.78
Bcl2l1	NM_009743	0.77
Casp7	NM_007611	0.76
Casp1	NM_009807	0.74
Trp53bp2	NM_173378	0.73
Atf5	NM_030693	0.72
Cideb	NM_009894	0.72
Casp3	NM_009810	0.71

Table W1. (*continued*)

Genes	GenBank	Fold Change KO/WT
Traf1	NM_009421	0.68
Traf2	NM_009422	0.65
Cradd	NM_009950	0.63
Birc5	NM_009689	0.62
Il10	NM_010548	0.55
Tnfsf10	NM_009425	0.54
Dsip1	NM_010286	0.51
Pycard	NM_023258	0.48
Bcl2	NM_009741	0.43
Trp53	NM_011640	0.41
Hells	NM_008234	0.24
Trp53inp1	NM_021897	0.20
Bcl2l10	NM_013479	No C_t
Casp14	NM_009809	No C_t
Cidea	NM_007702	No C_t
Lhx4	NM_010712	No C_t
Pak7	NM_172858	No C_t
Tnfsf5	NM_011616	No C_t
Tnfsf7	NM_011617	No C_t
Trp63	NM_011641	No C_t
Trp73	NM_011642	No C_t
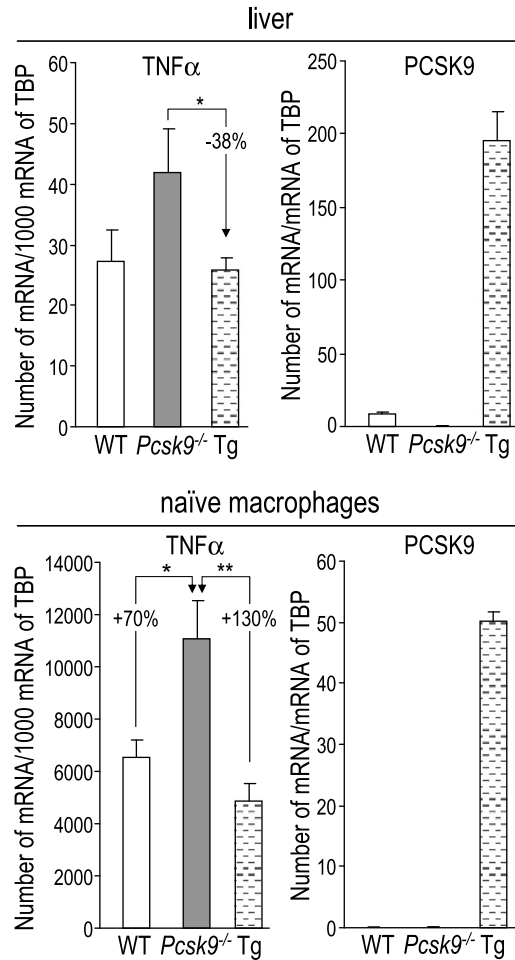
Figure W4. TNFα expression in livers and naïve macrophages. TNFα and PCSK9 expression was analyzed by qPCR in non-injected livers and naïve macrophages isolated from WT, $Pcsk9^{-/-}$, and PCSK9 transgenic (Tg) [11] mice (n = 6–10/genotype). Naïve macrophages were isolated from the mouse peritoneal cavity by lavaging with 10 ml of PBS. After centrifugation at low speed, the cell pellet was washed twice with 10 ml of PBS. Cells were then allowed to adhere to a plastic culture dish (35 mm) for 3 hours in RPMI 1640 containing 10% FBS. Non-adherent cells were washed off and adherent cells (essentially macrophages) were harvested for RNA extraction. Error bars indicate SEM. *P < .05 (Student's t test).